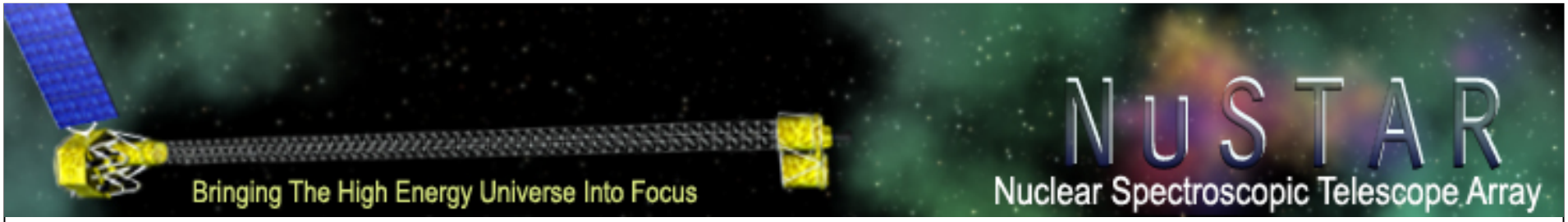

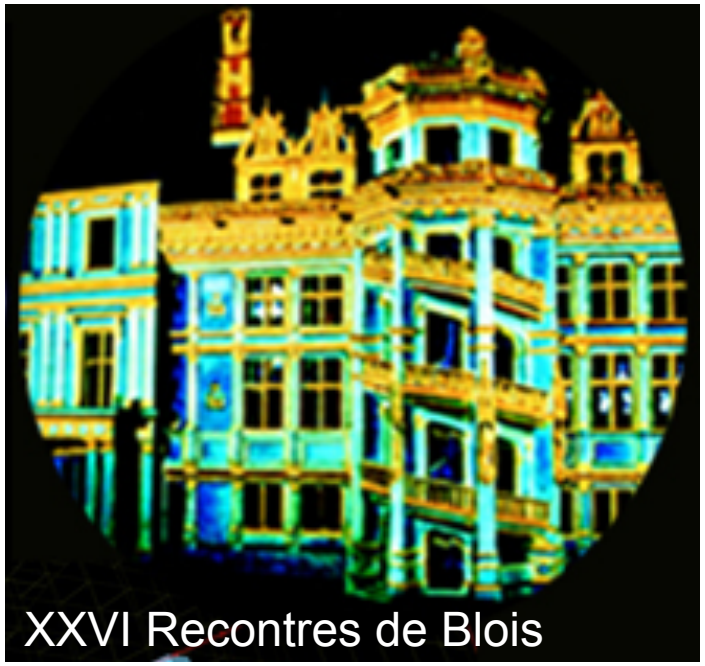

Results from the NuSTAR High-Energy X-ray Mission

Kerstin Perez

Columbia University

on behalf of the NuSTAR team

May 21, 2014

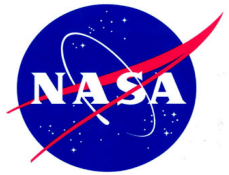

Outline

- Introducing *NuSTAR* and X-ray astrophysics
- Discovery of new source population in the Galactic Center
- Looking forward: NuSTAR and solar axions
- Conclusions

First high-energy X-ray focusing telescope in orbit

NuSTAR

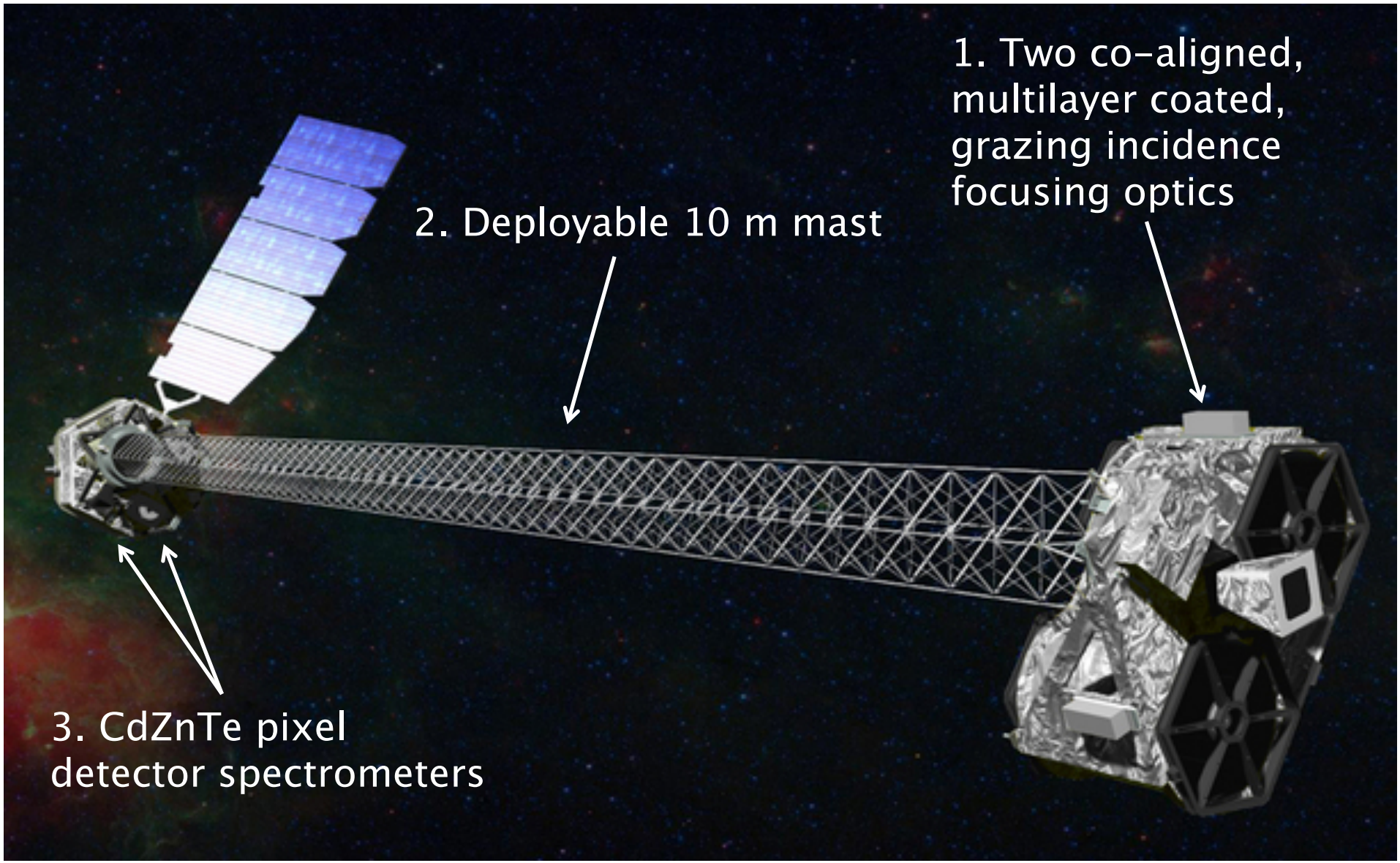

First high-energy X-ray focusing telescope in orbit

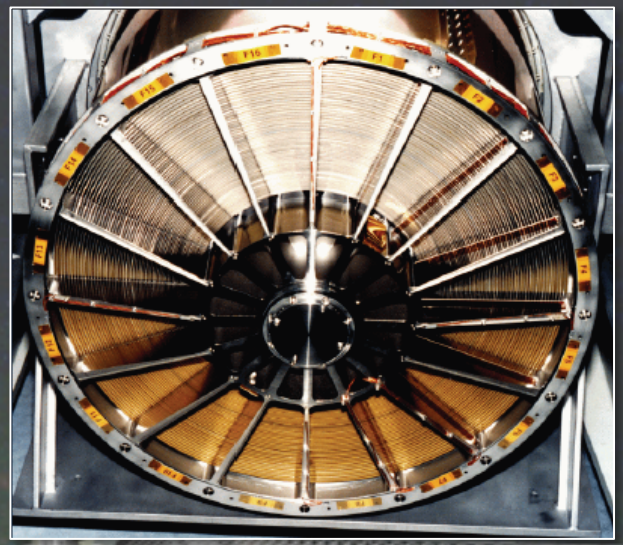

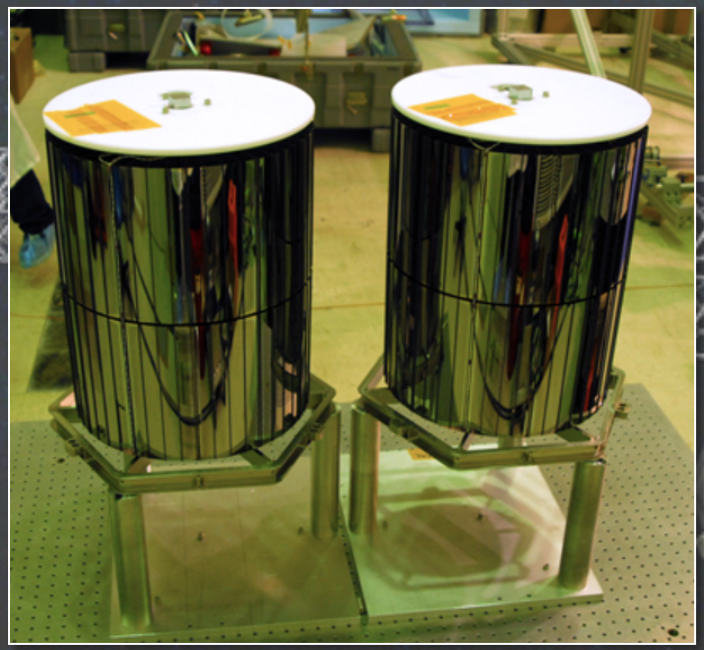

1. Two co-aligned, multilayer coated, grazing incidence focusing optics

From low to high-energy

NuSTAR

HUBBLE

HUBBLE + SPITZER

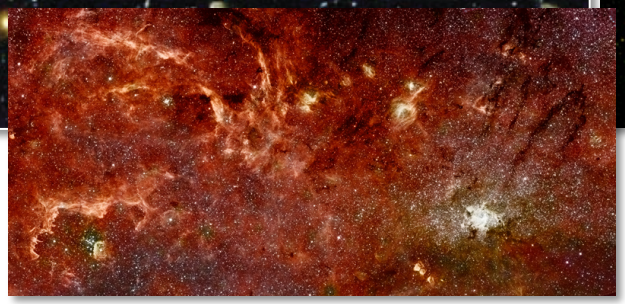

Stars and gas

NuSTAR + CHANDRA

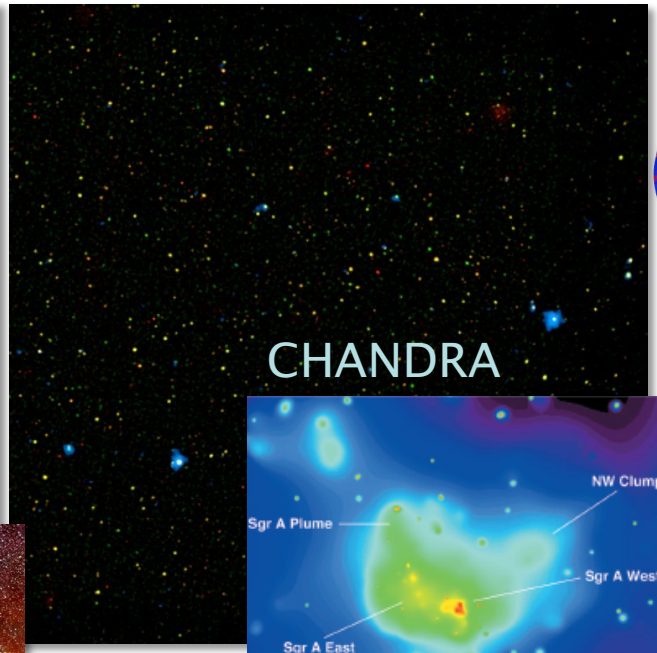

CHANDRA

Black holes, white dwarfs, neutron stars, supernovae, pulsars, scattering by cosmic rays

FERMI

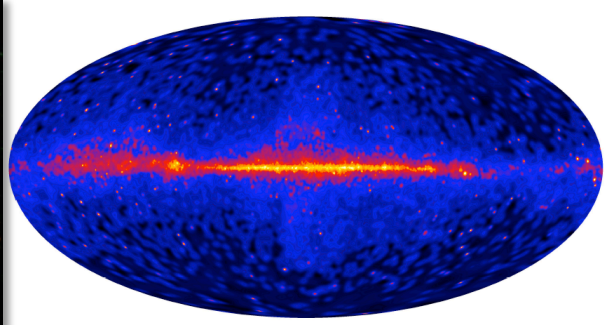

HESS

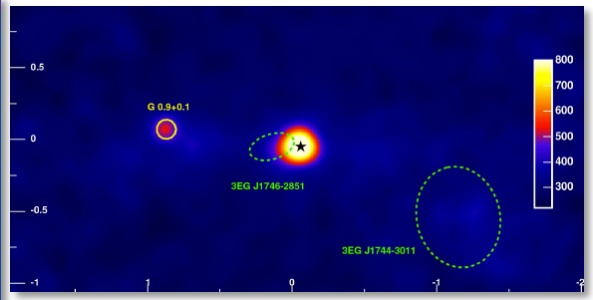

Pulsars, supernovae, AGN

NuSTAR telescope performance

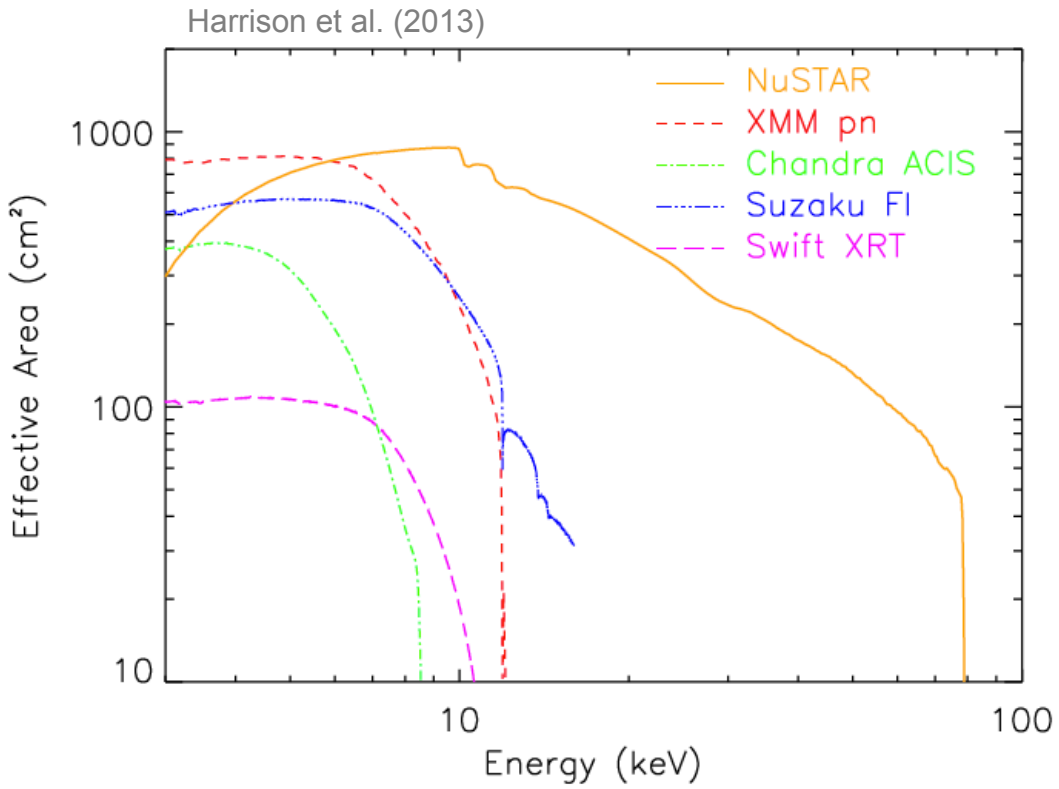

- **Energy Band:** 3–79 keV
- **Angular Resolution:**
  58" (HPD), 18" (PSF)
- **Field-of-view:** 12' x 12'
- **Energy resolution (FWHM):**
  0.4 keV at 6 keV,
  0.9 keV at 60 keV
- **Temporal resolution**: 0.1 ms
- **Maximum Flux Rate:** 10k cts/s
- **ToO response:** <24 hours

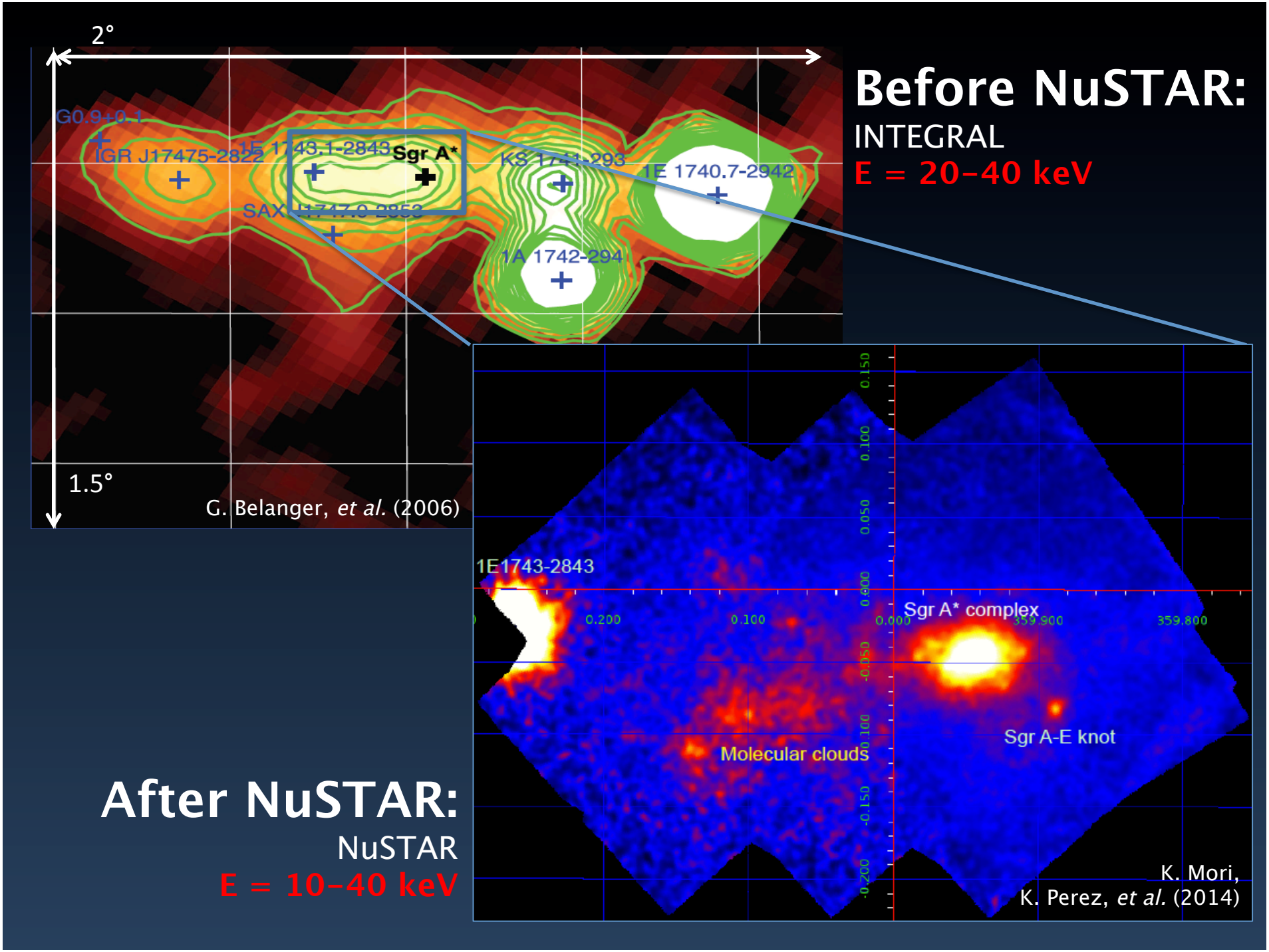
2°
1.5°
G0.9+0.1
IGR J17475-2822
1E 1743.1-2843
Sgr A*
SAX J1747.0-2853
KS 1741-293
1E 1740.7-2942
1A 1742-294
G. Belanger, et al. (2006)
Before NuSTAR:
INTEGRAL
E = 20-40 keV
1E1743-2843
Sgr A* complex
Molecular clouds
Sgr A-E knot
After NuSTAR:
NuSTAR
E = 10-40 keV
K. Mori,
K. Perez, et al. (2014)

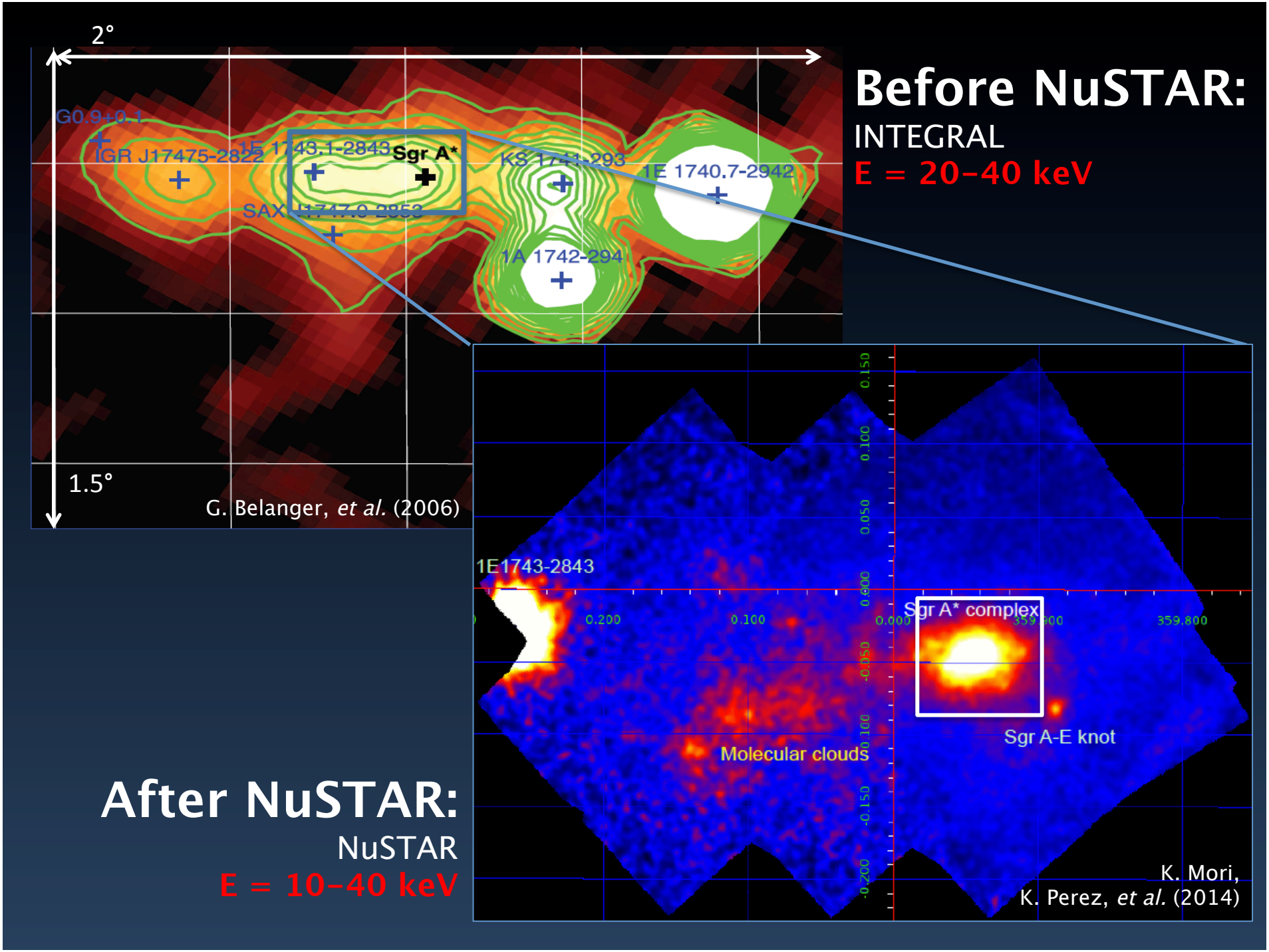
2°
1.5°
G0.9+0.1
IGR J17475-2822
1E 1743.1-2843
Sgr A*
SAX J1747.0-2853
KS 1741-293
1E 1740.7-2942
1A 1742-294
G. Belanger, et al. (2006)
Before NuSTAR:
INTEGRAL
E = 20-40 keV
1E1743-2843
Sgr A* complex
Sgr A-E knot
Molecular clouds
After NuSTAR:
NuSTAR
E = 10-40 keV
K. Mori,
K. Perez, et al. (2014)

*Inner 12 pc x 12 pc at **3-10 keV***

K. Mori, , K. Perez, *et al.* (2014)

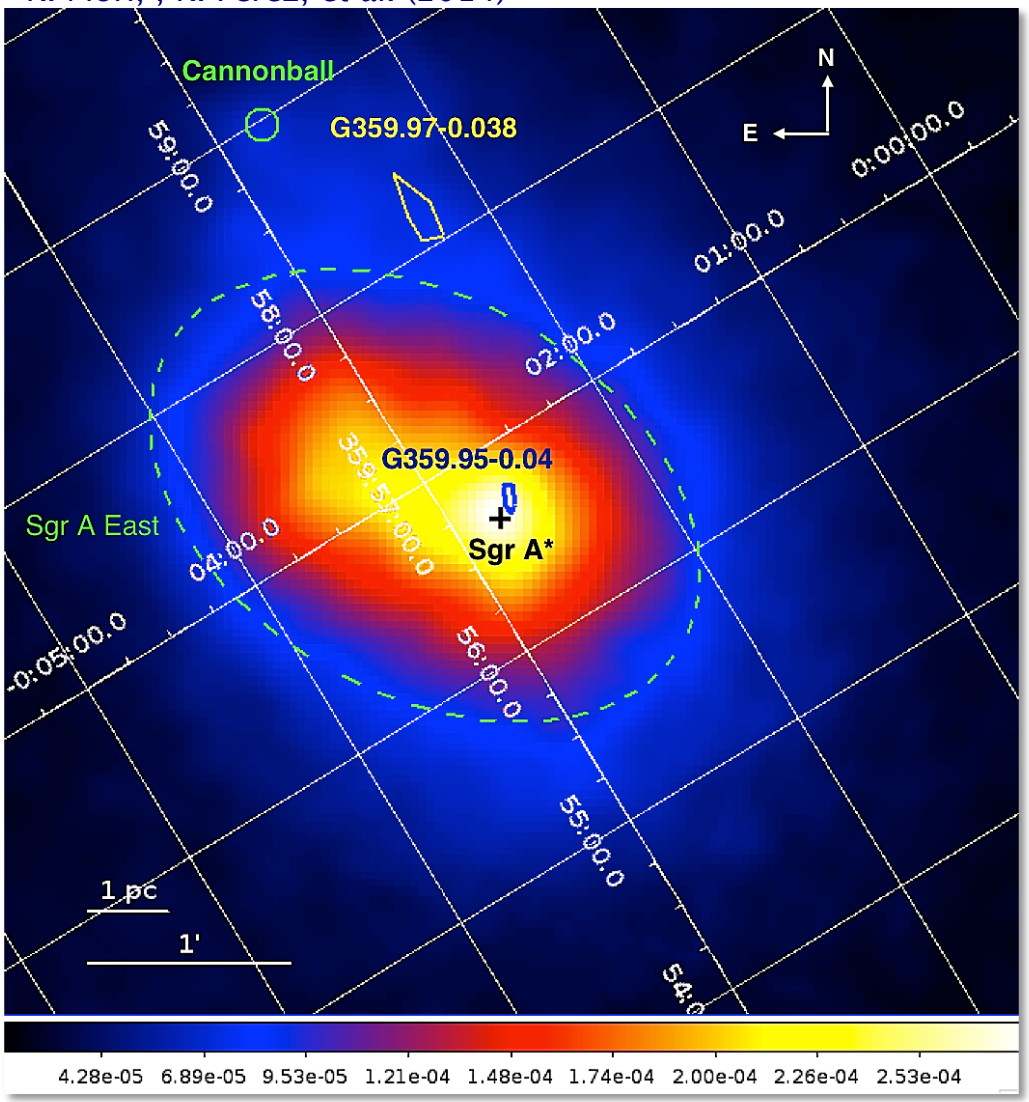

- The brightest emission (white) comes from the hot plasma surrounding Sgr A* and the pulsar wind nebula G359.95-0.04

- The surrounding emission (red and yellow) fills the shell of supernova remnant Sgr A East

- To the north-east lies the extended emission of the Sgr A-East “plume” (bright blue)

- The entire region sits in a field of diffuse and unresolved point source emission (dark blue)

*Inner 12 pc x 12 pc at **3-10 keV***

CHANDRA point sources - Muno *et al.* (2009)

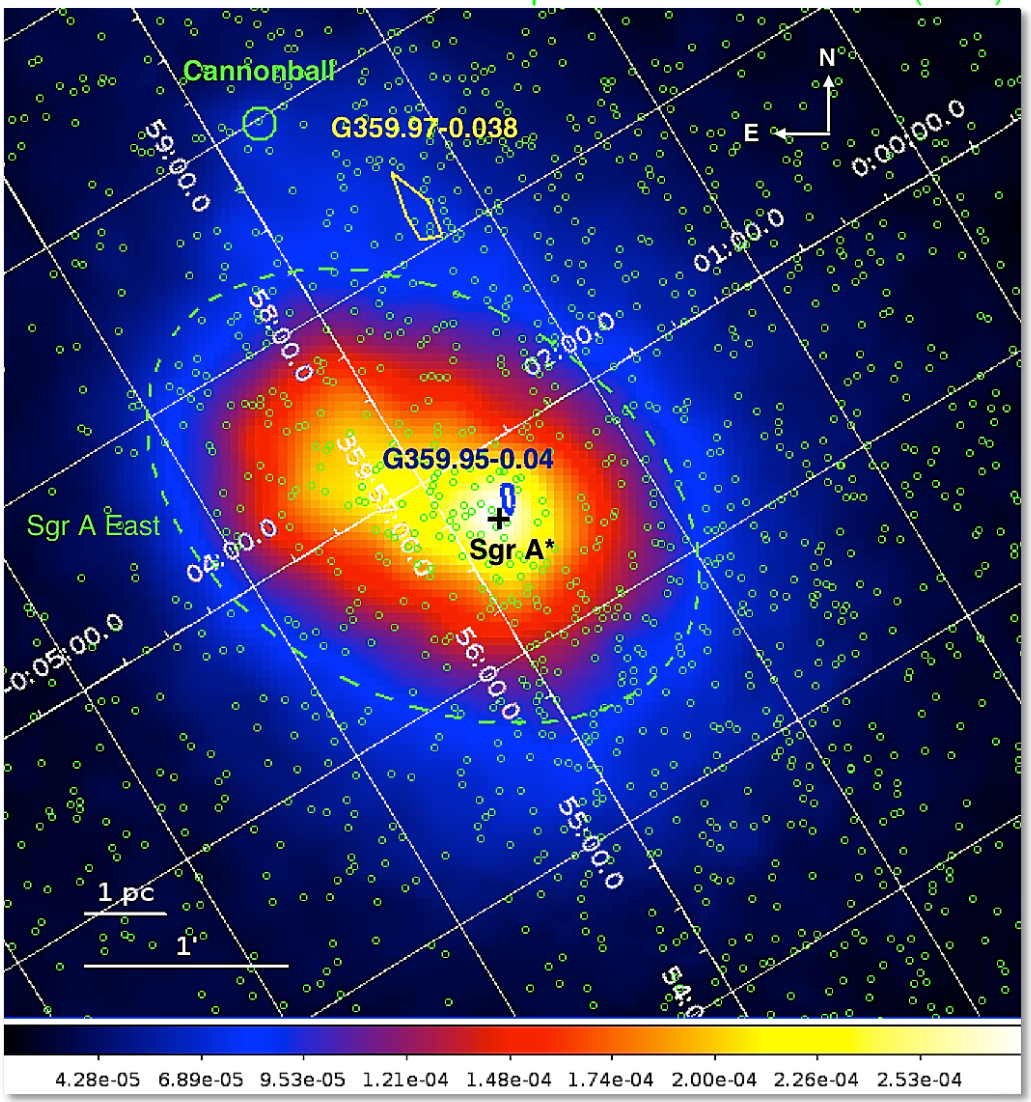

- The brightest emission (white) comes from the hot plasma surrounding Sgr A* and the pulsar wind nebula G359.95-0.04

- The surrounding emission (red and yellow) fills the shell of supernova remnant Sgr A East

- To the north-east lies the extended emission of the Sgr A-East “plume” (bright blue)

- The entire region sits in a field of diffuse and unresolved point source emission (dark blue)

*Inner 12 pc x 12 pc at **20-40 keV***

K. Perez, *et al.* (2014)

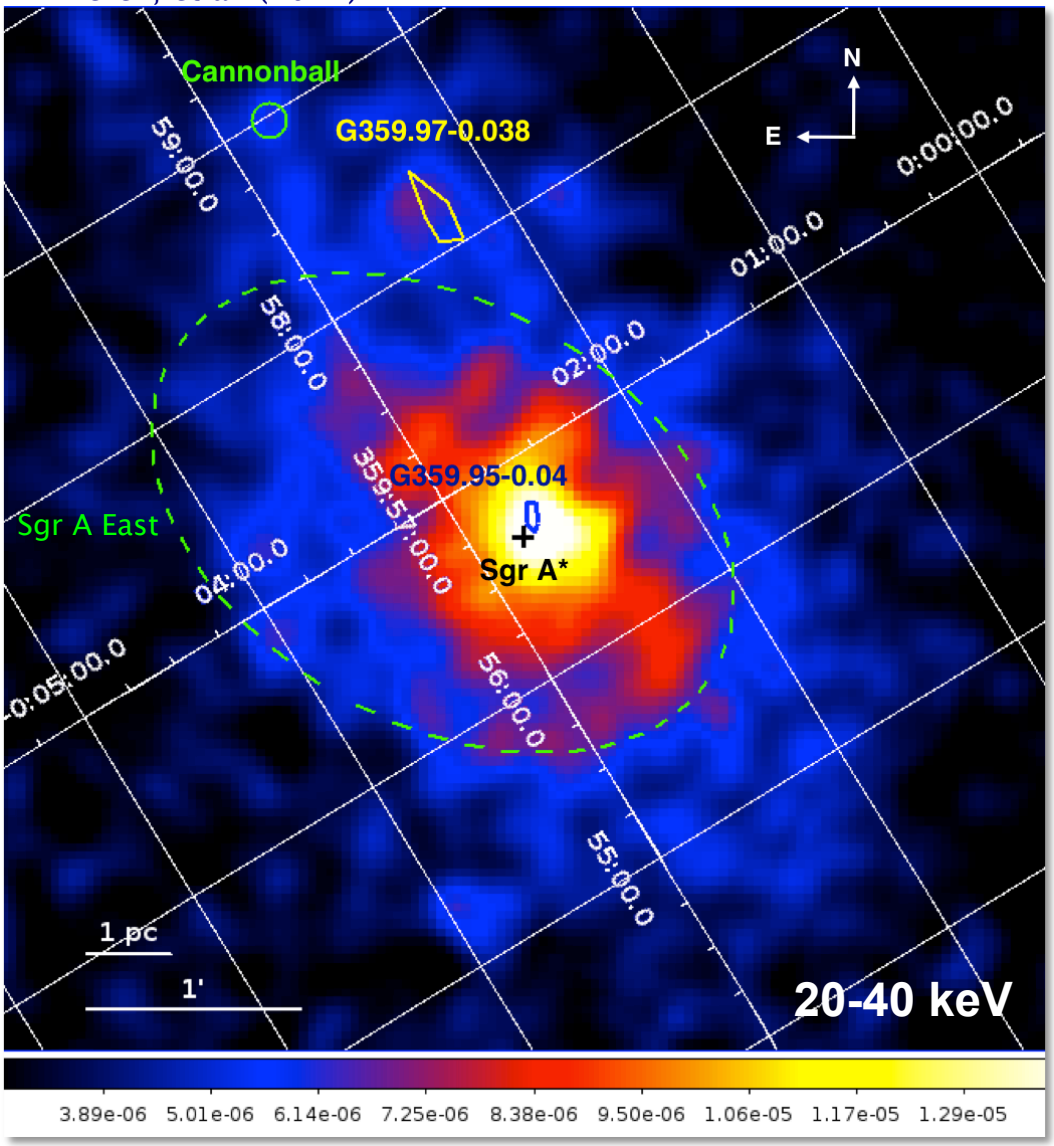

- Bright emission from pulsar wind nebula/Sgr A* region remains

- In addition, there is **a diffuse >20 keV X-ray emission extending along the Galactic plane from the Galactic Center**

*Inner 12 pc x 12 pc at **20-40 keV***

K. Perez, *et al.* (2014)

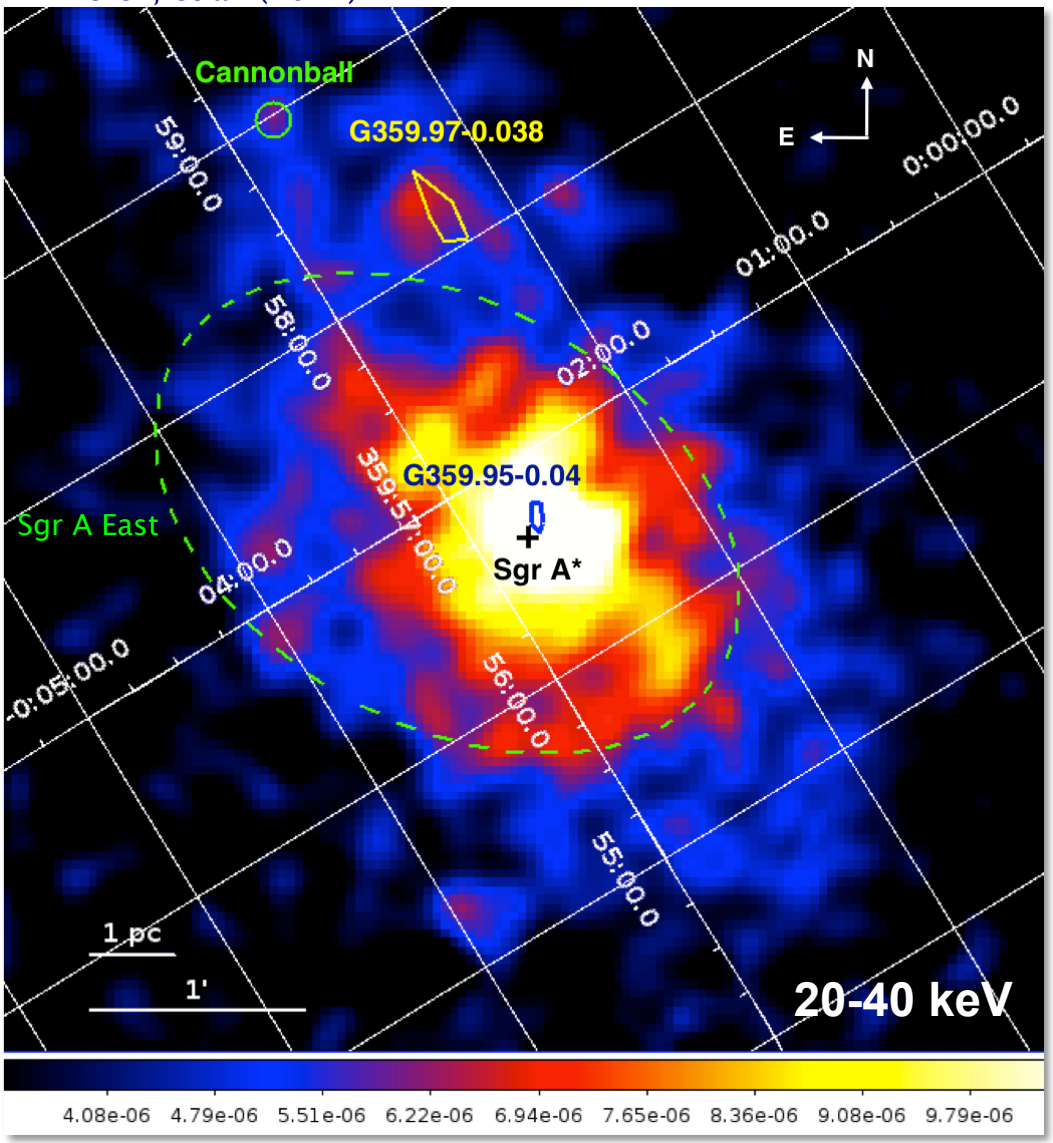

- Bright emission from pulsar wind nebula/Sgr A* region remains

- In addition, there is **a diffuse >20 keV X-ray emission extending along the Galactic plane from the Galactic Center**

New emission has 8 pc x 4 pc spatial extent

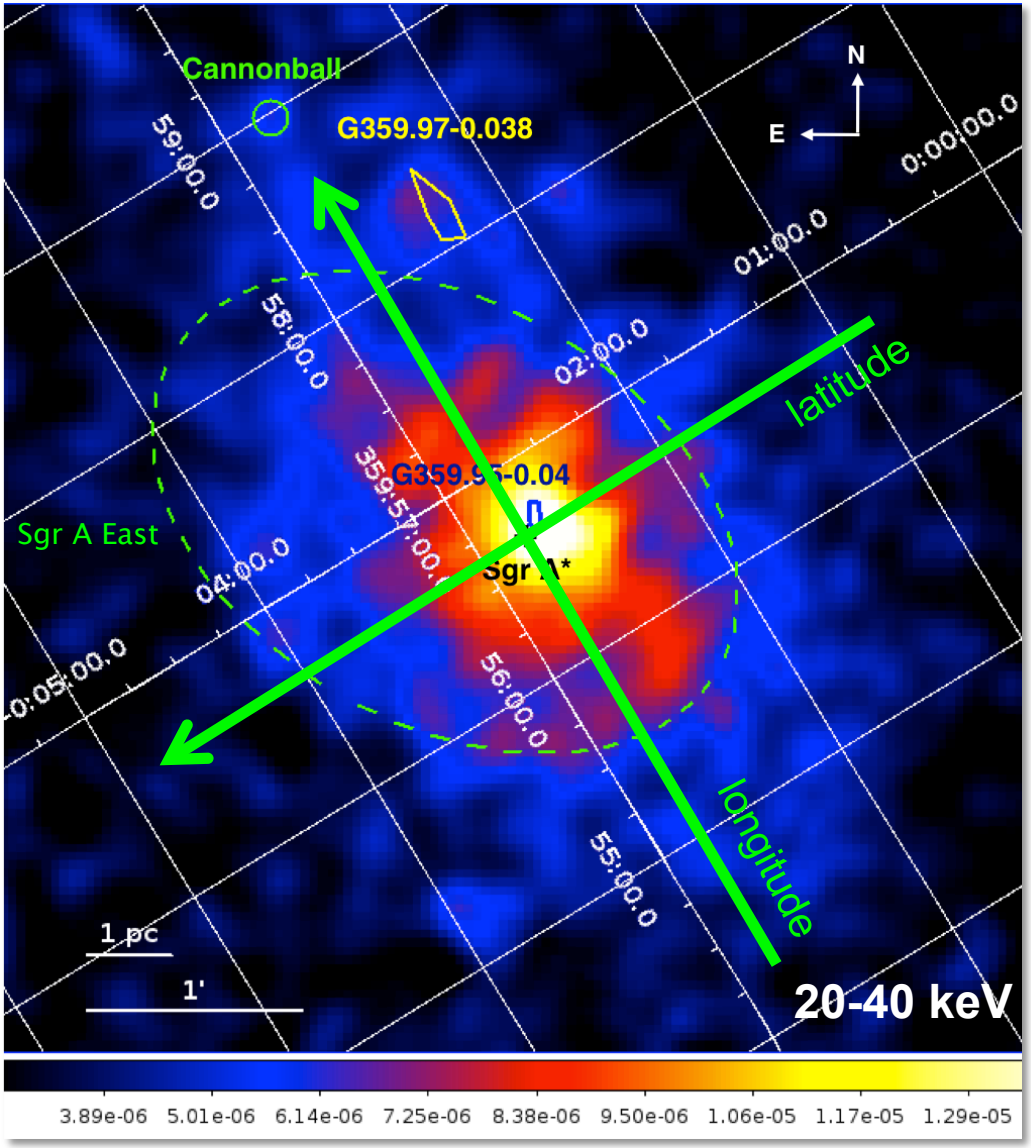

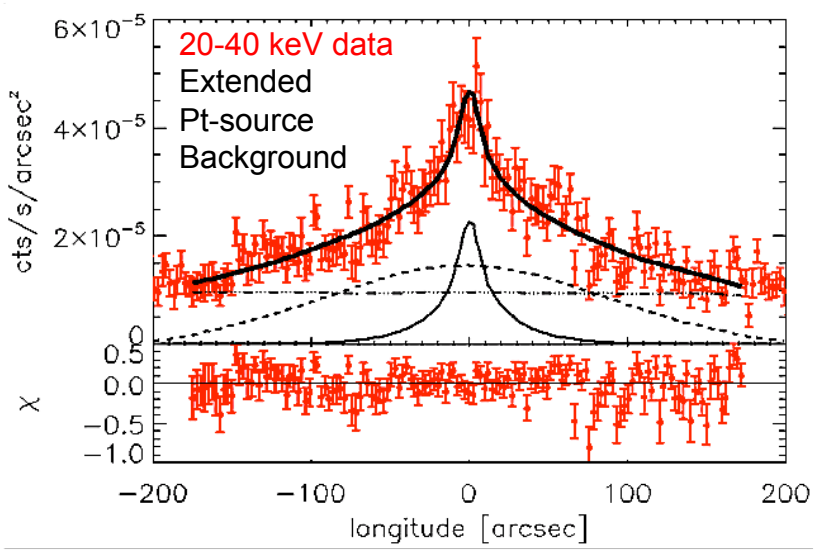

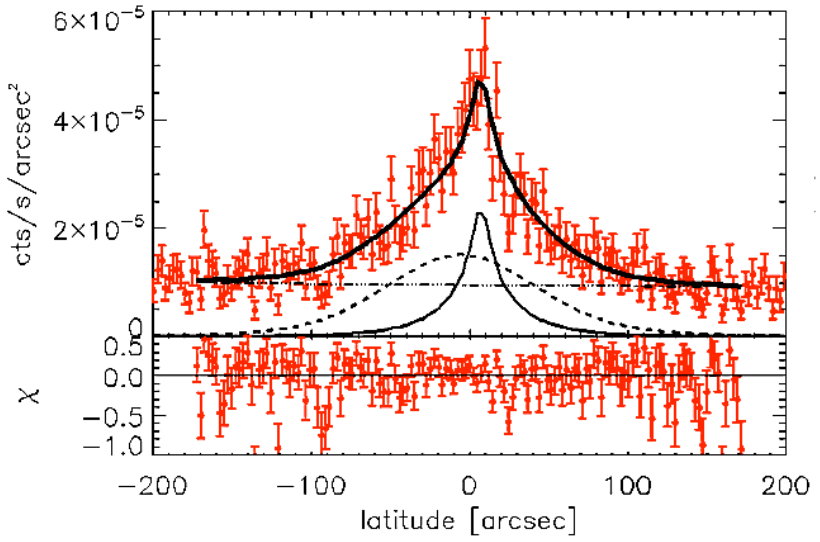

New emission has 8 pc x 4 pc spatial extent

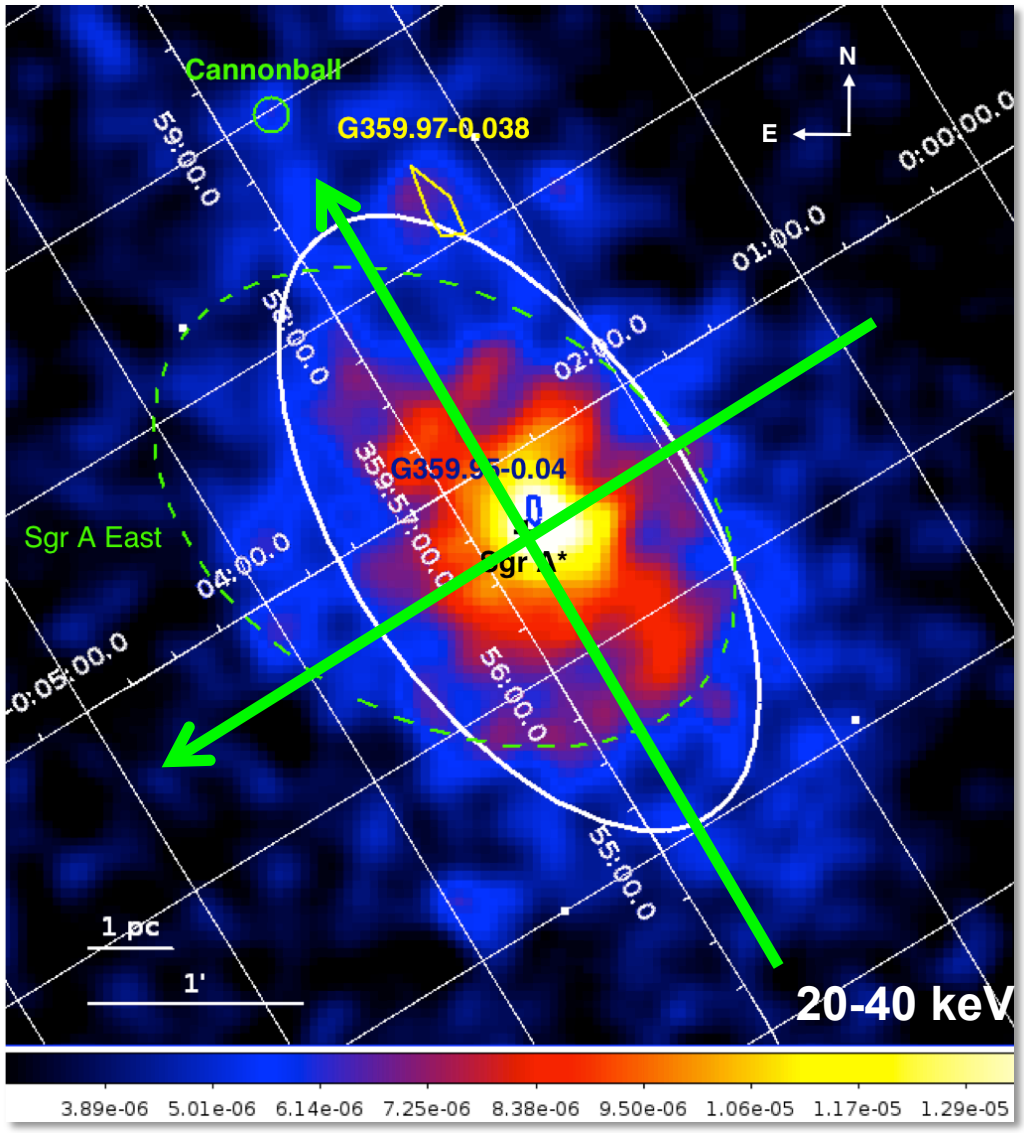

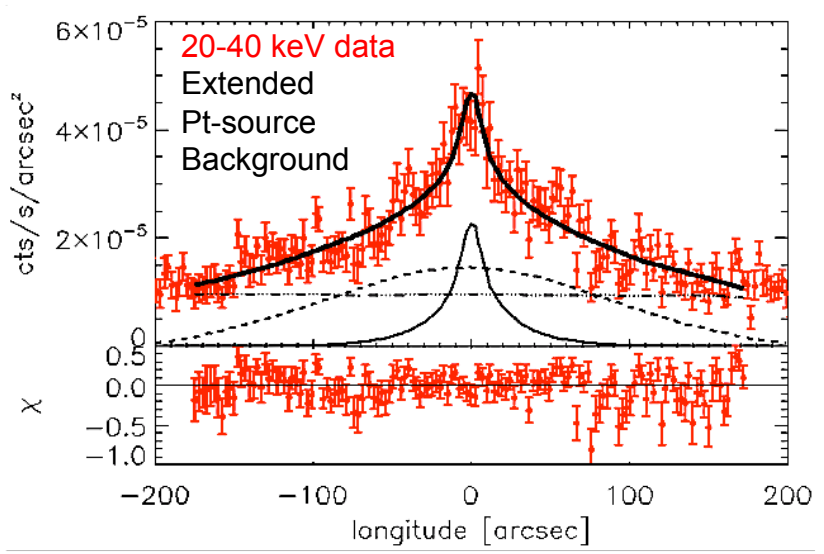

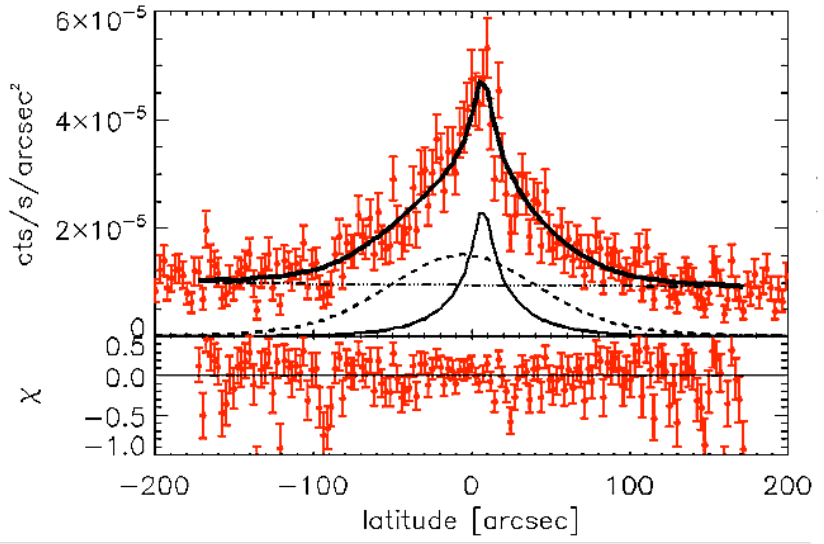

Either power-law with Γ ~ 1.6 or thermal with kT ~ 60 keV

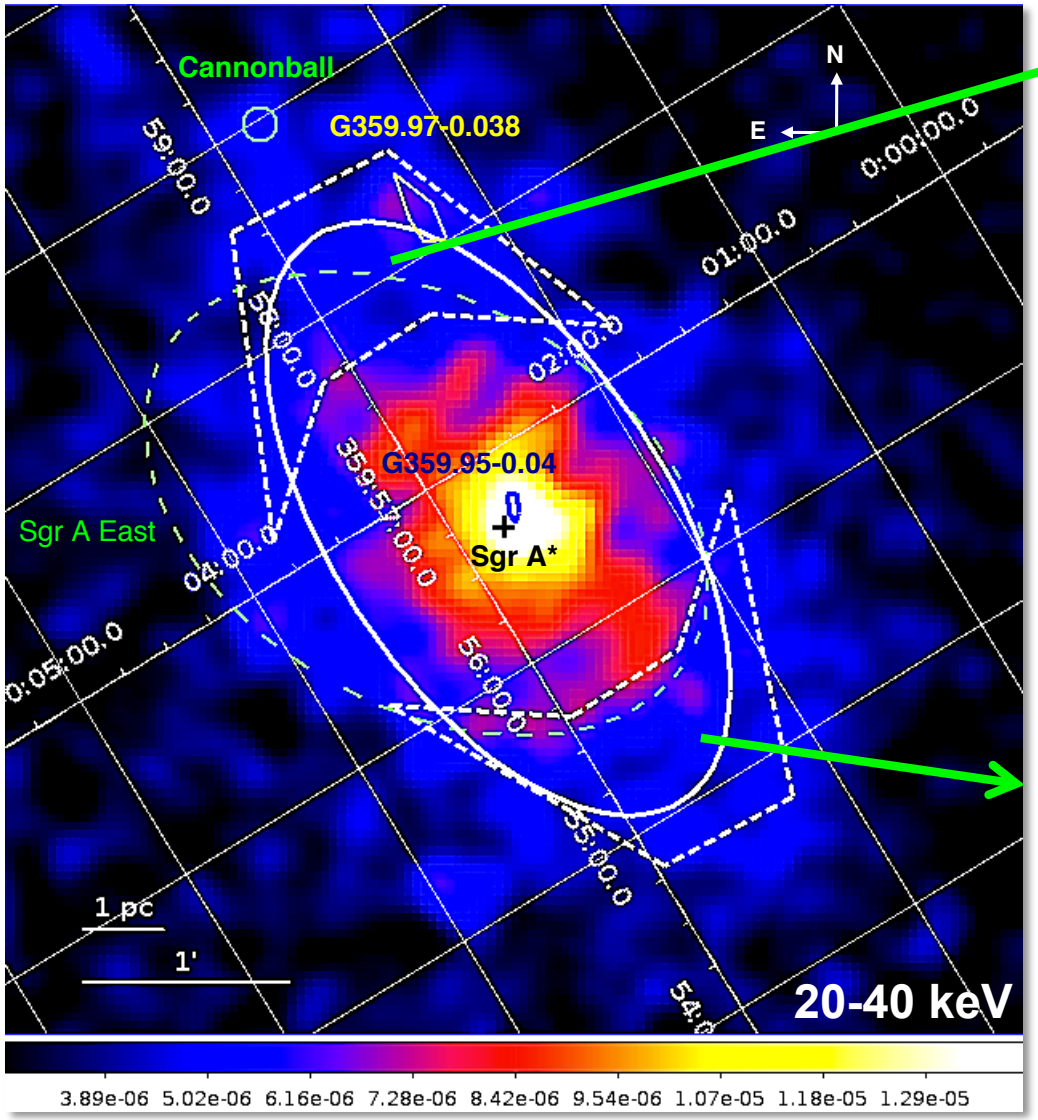

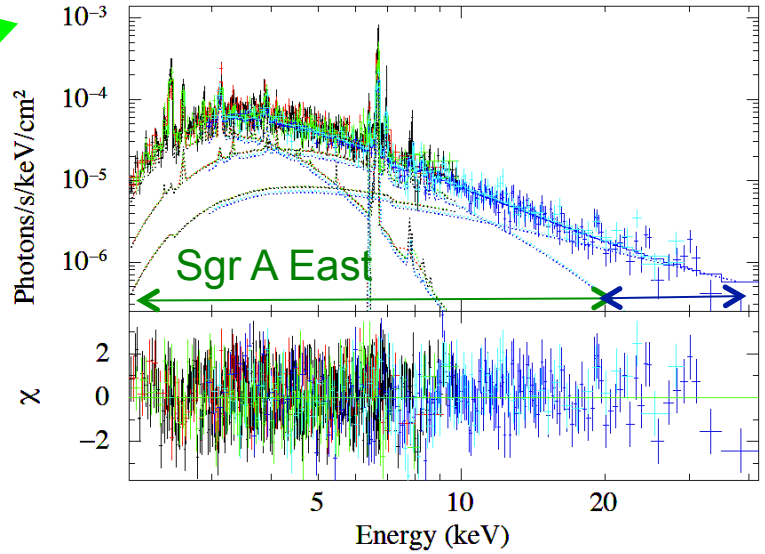

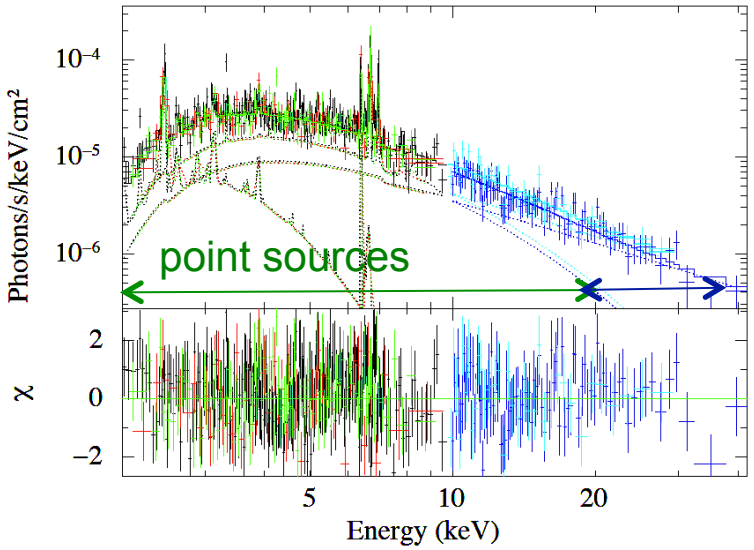

Origins of Diffuse Hard X-ray Emission (DHXE)

Any possible explanation of the DHXE must account for:

- symmetric along the Galactic plane around Sgr A*
- non-thermal with $\Gamma \approx 1.6$ or thermal with $kT \approx 60$ keV
- L(20-40 keV) $\approx 2.4 \times 10^{34}$ ergs/s within the 8 pc × 4 pc FWHM
- *transient limits from SWIFT monitoring*

Truly diffuse origins are ruled out. Possible explanations:

Scenario 1: Anomalously hot Intermediate Polars (IPs) with $kT \approx 60$ keV

- Much hotter and higher-mass white dwarf ($M > 1.0 M_O$) than previously observed populations

Scenario 2: Quiescent black hole low-mass X-ray binaries (qBH-LMXB)

- Previously undiscovered large population (~600-1200)
- Must have very faint or long-recurrence outburst

Scenario 3: Millisecond pulsars with non-thermal high-energy spectra

- Same population as could contribute gamma-ray dark matter signals!

Origins of Diffuse Hard X-ray Emission (DHXE)

"Regardless, the conclusion is that we are observing a vast graveyard of stellar remnants in the shadow of the supermassive black hole, posing significant theoretical challenges to our understanding of stellar evolution and binary formation in the Galactic Center"

Scenario 1: Anomalously hot Intermediate Polars (IPs) with kT ≈ 60 keV
- Much hotter and higher-mass white dwarf (M > 1.0M_O) than previously observed populations

Scenario 2: Quiescent black hole low-mass X-ray binaries (qBH-LMXB)
- Previously undiscovered large population (~600-1200)
- Must have very faint or long-recurrence outburst

Scenario 3: Millisecond pulsars with non-thermal high-energy spectra
- Same population as could contribute to FERMI dark matter signal!

Looking forward: NuSTAR and solar axions

- Axions are proposed to address the problem of particle physics CP-conservation of the strong force
- Dark Matter candidate with masses in range ~meV – μeV

Axions produced in Sun

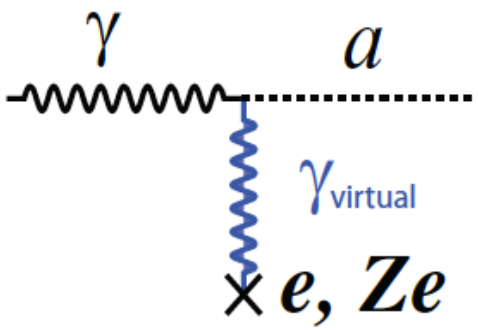

Converted back into photons by B-field

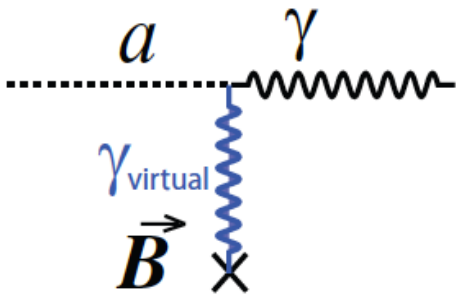

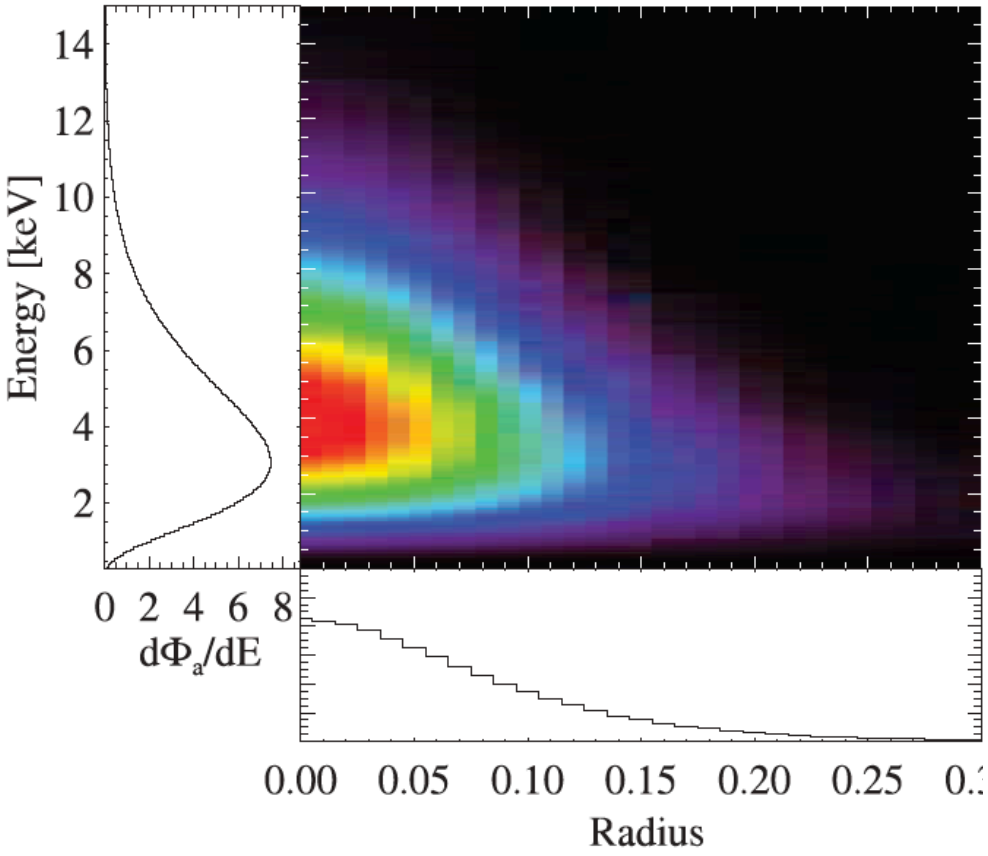

Conclusions

- NuSTAR is a powerful tool to probe high-energy processes in our universe

- NuSTAR has discovered a new population of high-energy X-ray sources in the Galactic Center, with implications for stellar evolution, binary formation, and dark matter searches

- X-rays are a potential probe of dark matter signatures

- NuSTAR has been approved for an extended mission through 2017, accepting observing proposals beginning end of this year

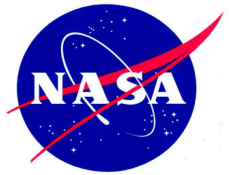

BACKUP

Hot Intermediate Polars ?

Scenario 1: Anomalously hot Intermediate Polars (IPs) with kT ≈ 60 keV

• much hotter than the kT ≈ 8 keV in the inner arcminutes (Muno 2004; Heard and Warwick 2012) or kT ≈15 keV observed in the inner Galactic bulge (Yuasa 2012)

• Swift, INTEGRAL, Suzaku, and XMM-Newton measurements of individual IPs show an average temperature of kT ≈ 20 keV, but exhibit a range in temperature from kT ≈ 10 keV to kT ≈ 90 keV

• Assume L_{min}(2-10 keV) ≈ 10^{30} – 10^{31} erg/s
L_{max}(2-10 keV) ≈ 10^{33} erg/s
α ≈ 1.0-1.5
→**800 – 8000 IPs in 8 pc × 4 pc**
→**6-60 IPs pc^{-3}**

• Observed spectrum implies white dwarf mass **M_{WD} > 1.0 M**

• Ensemble mass is significantly higher than that measured for mCVs in either the Galactic Center or bulge, though individual IPs with similar masses have been observed in the local solar neighborhood

Black hole low-mass X-ray binaries ?

Scenario 2: Quiescent black hole low-mass X-ray binaries (qBH-LMXB)

• Knowledge of the luminosity of qBH-LMXBs is limited to 10 known systems

• For L_{min}(2-10 keV) ≈ 2-4 × 10^{31} erg/s → 600-1200 qBH-LMXBs

• In the last decade, X-ray monitoring surveys uncovered virtually all transient systems within the inner 50 pc of the Galaxy with
  - recurrence times of < 5-10 years
  - outburst durations longer than a few days
  - outburst L(2-10 keV) > 10^{34} erg/s

→Typical qBH-LMXB with T_r ~ 50-100 years could make up at most 10% of DHXE

• Long T_r, long outburst BH-LMXB such as GRS 1915+105 also cannot dominate

• Fainter, non-transient BH-LMXB have been proposed (Menou 1999)(Casares 2014): the transition radius between the advection dominated accretion flow and the normal thin accretion disk is at large enough radius that the outer disk is always cool

Alternate populations

Although explanations in terms of hot IPs, qBH-LMXBs, or MSPs present challenges, other possible populations have been ruled out as majority contributors to the DHXE.

- **Neutron star LMXBs** have typical T_r ~ 5-10 years, would have been detected by Swift monitoring

- **Magnetars** with consistent spectra (soft gamma repeaters) have typical T_r ~ 10 years

- A large enough population of **non-thermal filaments** is not supported by Chandra or radio mapping of the Galactic center

- Low surface brightness **PWN** would require at least x10 higher PWN birth rate

- **Inverse Compton** from electrons injected from PWN, Sgr A*, colliding winds etc. scattering in the high radiation density of the center has a luminosity too low

- **Dark matter** does not reproduce spatial extent

Before NuSTAR:

INTEGRAL

E>15 keV

After NuSTAR:

NuSTAR

E = 3–79 keV

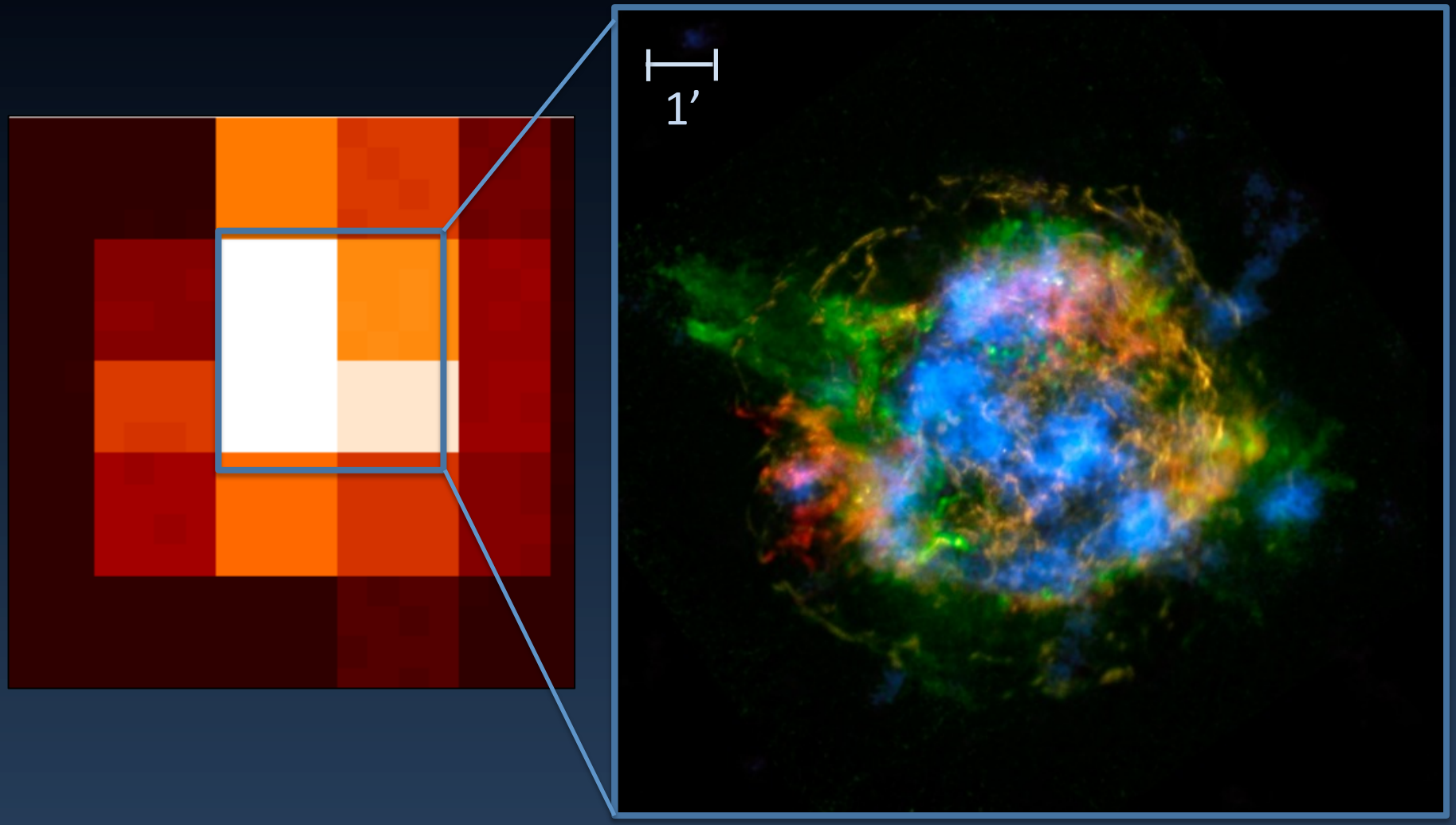

B. Grefenstette, *et al.* (2014)

Before NuSTAR:

INTEGRAL

E>15 keV

After NuSTAR:

NuSTAR

E ~ 67 keV

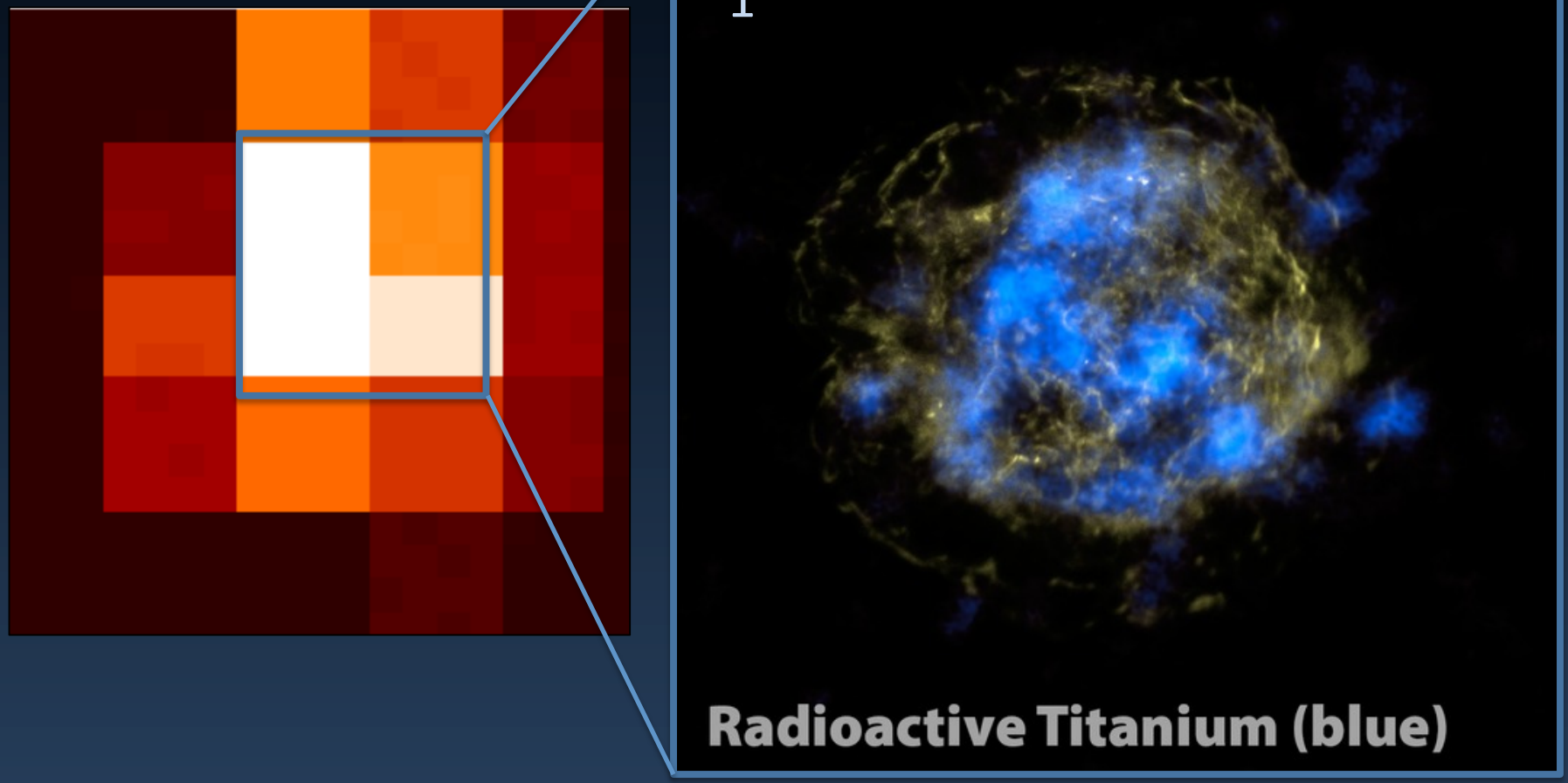

B. Grefenstette, *et al.* (2014)

20-40 keV Spatial Model

Supplementary Table 1: Parameters of the best-fit 2-D Gaussian models of the central source and the extended emission. The errors quoted are 3σ confidence levels. All parameters refer to source models before convolution with the NuSTAR PSF.

Parameter	Point source	Extended
R.A. (Center, J2000)	$266.4150^{\circ}{}^{+4.5''}_{-3.8''}$	$266.4172^{\circ}{}^{+6.6''}_{-6.2''}$
DEC (Center, J2000)	$-29.007245^{\circ}{}^{+3.4''}_{-4.1''}$	$-29.00716^{\circ}{}^{+8.1''}_{-7.1''}$
FWHM [arcseconds]	$1.8^{+2.3}_{-0.7}$	$195.8^{+21.9}_{-16.8}$
Amplitude [10^{-3} cts s^{-1}]	$5.2^{+7.1}_{-3.5}$	$0.0064^{+0.0012}_{-0.0017}$
Ellipticity	–	0.52
θ^{a} [degree]	–	57

[a] The angle θ is defined with respect to the positive northern axis.

Spectral Model

Supplementary Table 2: Spectral model of the two extended emission regions in the energy range 2-40 keV, obtained from joint fit of XMM (2-10 keV) and NuSTAR (10-40 keV) data, with the high-energy emission modeled as a power-law. All quoted errors are at 90% C.L.

Parameter	Southwest	Northeast
PN norm.[a]	$1.1^{+0.1}_{-0.1}$	$1.1^{+0.1}_{-0.1}$
MOS1 and MOS2 norm.	$1.0^{+0.1}_{-0.1}$	$1.1^{+0.1}_{-0.1}$
NuSTAR FPMA norm. (fixed)	1.0	1.0
NuSTAR FPMB norm.	$1.2^{+0.1}_{-0.1}$	$1.1^{+0.1}_{-0.1}$
N_H [10^{22} cm^{-2}]	$14.1^{+1.5}_{-1.3}$	$16.4^{+1.2}_{-0.8}$
Γ	$1.5^{+0.3}_{-0.2}$	$1.6^{+0.3}_{-0.4}$
N_Γ [10^{-4} photons cm^{-2} s^{-1} keV^{-1}]	$1.3^{+1.6}_{-0.7}$	$1.6^{+2.4}_{-1.1}$
kT_1 [keV]	$1.0^{+0.3}_{-0.4}$	$1.1^{+0.1}_{-0.2}$
N_{kT_1} [10^{-4} photons cm^{-2} s^{-1} keV^{-1}]	$10.8^{+103}_{-5.0}$	$89.9^{+56.1}_{-28.7}$
$Z_1[Z_\odot]$[b]	$5.0^{+--}_{-3.6}$	$2.3^{+0.9}_{-0.4}$
kT_2 [keV]	$7.5^{+1.6}_{-1.3}$	$5.1^{+0.9}_{-0.7}$
N_{kT_2} [10^{-4} photons cm^{-2} s^{-1} keV^{-1}]	$9.2^{+1.7}_{-1.6}$	$17.5^{+6.7}_{-5.9}$
$Z_2[Z_\odot]$[c]	1.7	$2.3^{+0.9}_{-0.4}$
Fe K-α eq. width [eV]	128^{+40}_{-31}	47^{+84}_{-16}
χ^2/d.o.f.	1.00 (503.4/503)	1.05 (807.1/770)
F_X (20-40 keV) [10^{-13} ergs cm^{-2} s^{-1}][d]	7.6	8.0

[a] Relative normalizations between different instruments, defined with respect to NuSTAR FPMA.

[b] Abundance relative to solar. These are best-fit values. In the southwest, Z_2 was then fixed during error calculations, as described in the text.

[c] Abundances are independent (linked) for the two temperature components in the southwest (northeast).

[d] Observed Flux.

Spectral Model

Supplementary Table 3: Spectral model of the two extended emission regions in the energy range 2-40 keV, obtained from joint fit of XMM (2-10 keV) and NuSTAR (10-40 keV) data, with the high-energy emission modeled as a thermal bremsstrahlung. All quoted errors are at 90% C.L.

Parameter	Southwest	Northeast
PN norm.[a]	$1.1^{+0.1}_{-0.1}$	$1.2^{+0.1}_{-0.1}$
MOS1 and MOS2 norm.	$1.1^{+0.1}_{-0.1}$	$1.2^{+0.1}_{-0.1}$
NuSTAR FPMA norm. (fixed)	1.0	1.0
NuSTAR FPMB norm.	$1.2^{+0.1}_{-0.1}$	$1.2^{+0.1}_{-0.1}$
N_H [10^{22} cm^{-2}]	$13.4^{+1.6}_{-1.3}$	$16.4^{+1.2}_{-0.8}$
kT_{bremss} [keV]	58^{+127}_{-23}	66^{+203}_{-30}
N_{bremss} [10^{-4} photons cm^{-2} s^{-1} keV^{-1}]	$1.8^{+0.4}_{-0.4}$	$1.9^{+0.4}_{-0.3}$
kT_1 [keV]	$1.0^{+0.3}_{-0.3}$	$1.1^{+0.1}_{-0.2}$
N_{kT_1} [10^{-4} photons cm^{-2} s^{-1} keV^{-1}]	$9.5^{+30}_{-2.0}$	$93.2^{+55.0}_{-22.2}$
Z_1 [$Z_\odot$][b]	$5.0^{+---}_{-3.2}$	$2.2^{+0.4}_{-0.3}$
kT_2 [keV]	$7.2^{+1.4}_{-1.3}$	$5.0^{+0.9}_{-0.7}$
N_{kT_2} [10^{-4} photons cm^{-2} s^{-1} keV^{-1}]	$8.8^{+2.0}_{-1.8}$	$18.0^{+6.1}_{-4.8}$
Z_2 [$Z_\odot$][c]	1.6	$2.2^{+0.4}_{-0.3}$
Fe K-α eq. width [eV]	123^{+90}_{-46}	46^{+12}_{-13}
χ^2/d.o.f.	1.00 (501.6/503)	1.05 (807.1/770)
F_X (20-40 keV) [10^{-13} ergs cm^{-2} s^{-1}][d]	7.3	8.0

[a] Relative normalizations between different instruments, defined with respect to NuSTAR FPMA.

[b] Abundance relative to solar. These are best-fit values. In the southwest, Z_2 was then fixed during error calculations, as described in the text.

[c] Abundances are independent (linked) for the two temperature components in the southwest (northeast).

[d] Observed Flux.

NuSTAR telescope performance

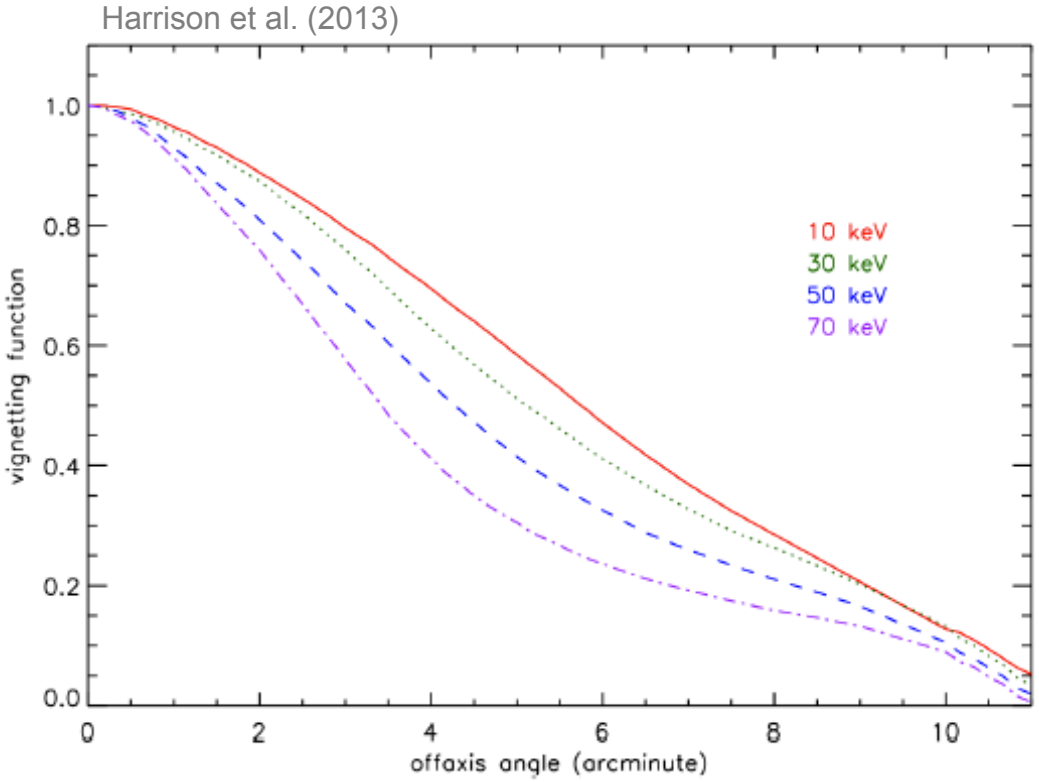

- **Energy Band:** 3–79 keV
- **Angular Resolution:**
  58" (HPD), 18" (PSF)
- **Field-of-view:** 12' x 12'
- **Energy resolution (FWHM):**
  0.4 keV at 6 keV,
  0.9 keV at 60 keV
- **Temporal resolution**: 0.1 ms
- **Maximum Flux Rate:** 10k cts/s
- **ToO response:** <24 hours

NuSTAR telescope performance

Satellite (instrument)	Sensitivity
INTEGRAL (ISGRI)	~0.5 mCrab (20-100 keV) with >Ms exposures
Swift (BAT)	~0.8 mCrab (15-150 keV) with >Ms exposures
NuSTAR	~0.8 μCrab (10-40 keV) in 1 Ms

- **Energy Band:** 3–79 keV
- **Angular Resolution:**
  58" (HPD), 18" (PSF)
- **Field-of-view:** 12' x 12'
- **Energy resolution (FWHM):**
  0.4 keV at 6 keV,
  0.9 keV at 60 keV
- **Temporal resolution**: 0.1 ms
- **Maximum Flux Rate:** 10k cts/s
- **ToO response:** <24 hours